Check for updates

Multi-isotopic analysis reveals the early stem turtle *Odontochelys* as a nearshore herbivorous forager

Jean Goedert[1]*, Romain Amiot[2], Jérémy Anquetin[3,4],
Nicolas Séon[1], Renaud Bourgeais[5], Gilles Bailly[6],
François Fourel[7], Laurent Simon[7], Chun Li[8], Wei Wang[8]
and Christophe Lécuyer[2]

[1]Muséum National d'Histoire Naturelle, Centre de Recherche en Paléontologie − Paris (CR2P), CNRS/MNHN/Sorbonne Université, Paris, France, [2]Univ Lyon, Université Claude Bernard Lyon 1, CNRS, ENSL, UJM, LGL-TPE, Villeurbanne, France, [3]JURASSICA Museum, Porrentruy, Switzerland, [4]Department of Geosciences, University of Fribourg, Fribourg, Switzerland, [5]Université PSL − Ecole Pratique des Hautes Etudes, Les Patios Saint-Jacques, Paris, France, [6]Musée d'Angoulême, Angoulême, France, [7]Univ Lyon, Université Claude Bernard Lyon 1, CNRS, ENTPE, UMR 5023 LEHNA, Villeurbanne, France, [8]Key Laboratory of Vertebrate Evolution and Human Origins of Chinese Academy of Sciences, Institute of Vertebrate Paleontology and Paleoanthropology, Beijing, China

Introduction: After decades of debate on the origin of turtles, it is now widely accepted that they are diapsid reptiles originating in the Permian from a terrestrial ancestor. It seems that the initial development of the structures that will later form the unique turtle bony shell took place as a response to a fossorial lifestyle. However, the earliest stem turtle with a fully complete plastron, *Odontochelys semitestacea* from the Late Triassic (lower Carnian) of China, is somewhat controversially interpreted as an aquatic or even a marine form, raising the question of the environment in which the completion of the plastron happened.

Methods: Here, we analyzed the stable carbon, oxygen and sulfur isotope compositions ($\delta^{13}C$, $\delta^{18}O$ and $\delta^{34}S$) of bones from two specimens of *Odontochelys* along with bones and teeth of two associated specimens of the marine ichthyosaur *Guizhouichthyosaurus tangae*.

Results and discussion: We first show that $\delta^{18}O$ values of *Odontochelys* are incompatible with a terrestrial lifestyle and imply a semi-aquatic to aquatic lifestyle. Isotopic results also demonstrate that the aquatic environment of *Odontochelys* was submitted to a strong marine influence, therefore excluding the possibility of a strict freshwater aquatic environment. Additionally, an unusual carbon isotope composition shows that *O. semitestacea* was herbivorous, probably consuming macrophytic algae in coastal zones like the extant green sea turtle (*Chelonia mydas*) or the marine iguana (*Amblyrhynchus cristatus*) do.

KEYWORDS

Triassic, sulfur, oxygen, carbon, geochemistry, paleoecology, vertebrate

Introduction

The paleoecology of early turtles long remained obscure and contentious. Did the turtle shell, a novel and unique morphological structure, evolve in a terrestrial or aquatic context? Many paleontologists used to place turtles close to various groups of mainly terrestrial early reptiles (procolophonids, pareiasaurs), now usually referred to Parareptilia, which suggested a terrestrial origin for turtles (e.g., Laurin and Reisz, 1995; Lee, 1997; Lyson et al., 2010; Lichtig and Lucas, 2021). In contrast, other authors favored a relationship with Sauropterygia, which suggested a marine or aquatic origin for the group (Rieppel and deBraga, 1996; deBraga and Rieppel, 1997; Rieppel and Reisz, 1999; Schoch and Sues, 2015; Li et al., 2018). The description of *Odontochelys semitestacea*, a Late Triassic stem turtle from China characterized by the presence of an incompletely formed shell and interpreted to inhabit marginal areas or river deltas, seemed at first to confirm the aquatic origin of turtles (Li et al., 2008). However, the incomplete carapace of *Odontochelys* formed in part by anteroposteriorly broadened ribs prompted a renewed interest into the enigmatic Permian reptile *Eunotosaurus africanus*, which presents a similar morphology (Lyson and Bever, 2020; Schoch and Sues, 2020). A series of studies subsequently established a convincing link between *Eunotosaurus*, turtles, and diapsid reptiles (Lyson et al., 2010; Lee, 2013; Lyson et al., 2013; Lyson et al., 2014; Bever et al., 2015; Bever et al., 2016; Lyson et al., 2016), and this link was later substantiated by the description of *Pappochelys rosinae* and *Eorhynchochelys sinensis* (Schoch and Sues, 2015; Li et al., 2018). It is important to note here that the vast majority of molecular studies converged during the same time upon a turtle and archosaur relationship (e.g., Joyce, 2015; Gemmell et al., 2020). It seems that most paleontologists now agree that turtles are diapsid reptiles, and that, at least early on, the origin of the turtle shell (notably the broadened trunk ribs) is probably linked to a fossorial lifestyle (Lyson et al., 2016; Schoch et al., 2019; Lyson and Bever, 2020). In this context, the paleoecology of *Odontochelys*, the earliest stem turtle to exhibit a fully formed plastron, is an information of major importance.

Odontochelys remains were found in the marine sediments of the lower member of the Xiaowa Formation, deposited in the Nanpanjiang Trough Basin, near Guanling in Guizhou Province, China (Li et al., 2008). At the time of their deposition (early to middle Carnian), the basin was surrounded by emergent areas on three sides only opening southward-westward into the Paleotethys (Wang et al., 2008). The authors concluded that *Odontochelys* inhabited marginal areas of the seas or river deltas (Li et al., 2008), but morphological features supporting this interpretation are lacking (e.g., Joyce, 2015; Schoch et al., 2019). Paleoecological models tend to suggest that *Odontochelys* was probably an aquatic taxon, but maybe not a marine one (Li et al., 2008; Joyce, 2015; Lichtig and Lucas, 2017; Dudgeon et al., 2021). Rothschild and Naples (2015) identified evidence of decompression syndrome in *Odontochelys*, which suggests an aquatic lifestyle. Hence, the paleoecology of *Odontochelys* remains hitherto unclear.

Stable isotope analyses of bioapatite minerals that constitute the skeletons of vertebrates have been widely used to investigate the ecology of fossil taxa (e.g., Martin et al., 2017). More recently, some

isotopic systems proved to be of particular interest to trace the salinity of the living aquatic environment of vertebrates (Goedert et al., 2018; Goedert et al., 2020; Thibon et al., 2022). Here, we analyzed the stable carbon and oxygen isotope compositions of structural carbonate ($\delta^{13}C_c$ and $\delta^{18}O_c$), the stable oxygen isotope composition of phosphate ($\delta^{18}O_p$) and the stable sulfur isotope composition ($\delta^{34}S$) of bioapatite of *Odontochelys* in order to investigate its ecology in terms of feeding behavior and living environment. Carbon isotope composition was more specifically used as a dietary tracer (e.g., Clementz and Koch, 2001; Biasatti, 2004; Clementz et al., 2007), while the conjoint analysis of oxygen and sulfur isotope compositions was used as a tracer of the salinity of the environment in which lived *Odontochelys* (Goedert et al., 2018, 2020). The stable isotope compositions of ichthyosaur specimens from the same geological horizon and locality were also analyzed to serve as a marine reference.

Results

The modern carnivorous sea turtle species (*Lepidochelys olivacea*; *Dermochelys coriacea* and *Caretta caretta*) have significantly (Mann-Whitney U: *p-value* = 0.00002) lower $\delta^{13}C_c$ values than the modern herbivorous sea turtle species, marine iguana and dugong (*Chelonia mydas*, *Amblyrhynchus cristatus* and *Dugong dugon*; Supplementary Table 1; Figure 1). The two specimens of *Odontochelys* have significantly higher $\delta^{13}C_c$ values than those of *Guizhouichthyosaurus* (Mann-Whitney U: *p-value* = 0.036; Supplementary Table 1; Figure 1). Both specimens of *Odontochelys* have positive $\delta^{13}C_c$ values, like some modern *C. mydas* individuals do. The two Mesozoic marine turtles (*Jurassichelon oleronensis* and Chelonioidea indet.) have $\delta^{13}C_c$ values intermediate between those of *Guizhouichthyosaurus* and *Odontochelys* ($\delta^{13}C_c = -3.27$ ‰ and -0.68 ‰).

The modern terrestrial turtle *Testudo kleinmanni* has the most elevated $\delta^{18}O_p$ values ($\delta^{18}O_p = +24.2$ ‰, Supplementary Table 1 and calculated $\delta^{18}O_w$ values, see Figure 2; Supplementary Table 2). Modern marine turtles and iguana also have elevated $\delta^{18}O_p$ values that are significantly (Mann-Whitney U: *p-value* = 0.02381) higher than those of modern freshwater turtles (Supplementary Table 2; see also Figure 2 for calculated $\delta^{18}O_w$ values). *Odontochelys* specimens have $\delta^{18}O_p$ values similar to those of *Guizhouichthyosaurus* ($\delta^{18}O_p = +19.4 \pm 0.4$ ‰ vs $\delta^{18}O_p = +19.3 \pm 0.2$ ‰; Mann-Whitney U: *p-value* = 0.85714; Supplementary Table 1). These values are slightly lower than those of modern marine turtles and iguana although the difference is not significant (Mann-Whitney U: *p-value* = 0.1). Both the Mesozoic marine turtles *J. oleronensis* and Chelonioidea indet. have elevated $\delta^{18}O_p$ values ($\delta^{18}O_p = +20.9$ ‰ and $+20.2$ ‰, respectively) comparable to that of *Odontochelys* and *Guizhouichthyosaurus*. The two specimens of *Odontochelys* have similar $\delta^{18}O_p$ values of $+19.2 \pm 0.2$ ‰ (n = 2; IVPP V 15653) and $+19.8$ ‰ (IVPP V 13240). The two specimens of *Guizhouichthyosaurus* have also similar $\delta^{18}O_p$ values ($+19.2 \pm 0.1$ ‰ (n = 3; IVPP V 11865) and $+19.4 \pm 0.4$ ‰ (n = 2; IVPP V 11869); Supplementary Table 1).

The modern terrestrial turtle *Testudo kleinmanni* has a rather high $\delta^{34}S$ value of $+17.0$ ‰, which may be due to the coastal

FIGURE 1

Stable carbon isotope composition of bioapatite carbonate of *Odontochelys* (dark green dots), compared to the marine carnivorous ichthyosaur *Guizhouichthyosaurus* (dark blue squares), two Mesozoic marine turtles (grey dots), the modern marine dugong (*D. dugon*; light green star), the modern marine iguana (*A. cristatus*; light green diamond) and modern turtle species of different ecologies: *C. mydas* (marine, herbivorous; light green dots) and *L. olivacea*, *D. coriacea* and *C. caretta* (marine, carnivorous; light orange dots). The $\delta^{13}C_c$ values of *D. dugon* are from MacFadden et al. (2004), those of *A. cristatus* (n = 5) and *C. caretta* (n = 5) are from Wheatley et al. (2012), and those of *C. mydas*, *L. olivacea* and *D. coriacea* are from Biasatti (2004). Each error bar corresponds to 1 s.d. (Supplementary Table 1).

location of its habitat (Supplementary Table 1; Figure 2). Both specimens of modern marine turtles *C. mydas* have elevated $\delta^{34}S$ values of + 22.9 ‰ and + 19.5 ‰. These values are higher than the $\delta^{34}S$ values of modern freshwater turtles that range from + 6.7 ‰ to + 16.3 ‰. *Guizhouichthyosaurus* sample ICHTH-5 has an elevated $\delta^{34}S$ value of + 19.2 ‰ comparable to the modern marine turtle ones. *Odontochelys* sample OD-2 has a $\delta^{34}S$ value of + 15.3 ‰ intermediate between those of modern freshwater turtles and those of modern marine turtles and *Guizhouichthyosaurus* sample ICHTH-5. When considered conjointly, the $\delta^{18}O_w$ and $\delta^{34}S_w$ values of *Odontochelys* sample OD-2 (and even OD-3, but see Discussion section) falls intermediate between those of modern freshwater turtles and marine taxa (modern marine turtles and

Guizhouichthyosaurus sample ICHTH-5 (as well as ICHTH-1, 3 and 4, but see Discussion section; Figure 2).

Samples of *Odontochelys* and *Guizhouichthyosaurus*, that display the lowest sulfur content, have high $\delta^{34}S$ values (Supplementary Table 1; Figure 3). *Odontochelys* and *Guizhouichthyosaurus* have $\delta^{34}S$ values that display respectively a non-significant ($R^2 = 0.95$; *p-value* = 0.139; n = 3) and significant ($R^2 = 0.90$; *p-value* = 0.0136; n = 5) positive correlation with the inverse of the sulfur concentration (Figure 3). The marine Cretaceous turtle Chelonioidea indet., which has a negative $\delta^{34}S$ values of − 1.3 ‰, has also the highest sulfur content (2.33 %; Supplementary Table 1; Figure 3). This is similar to the *Odontochelys* sample OD-4, which also has a low, negative, $\delta^{34}S$ value associated with relatively high sulfur content
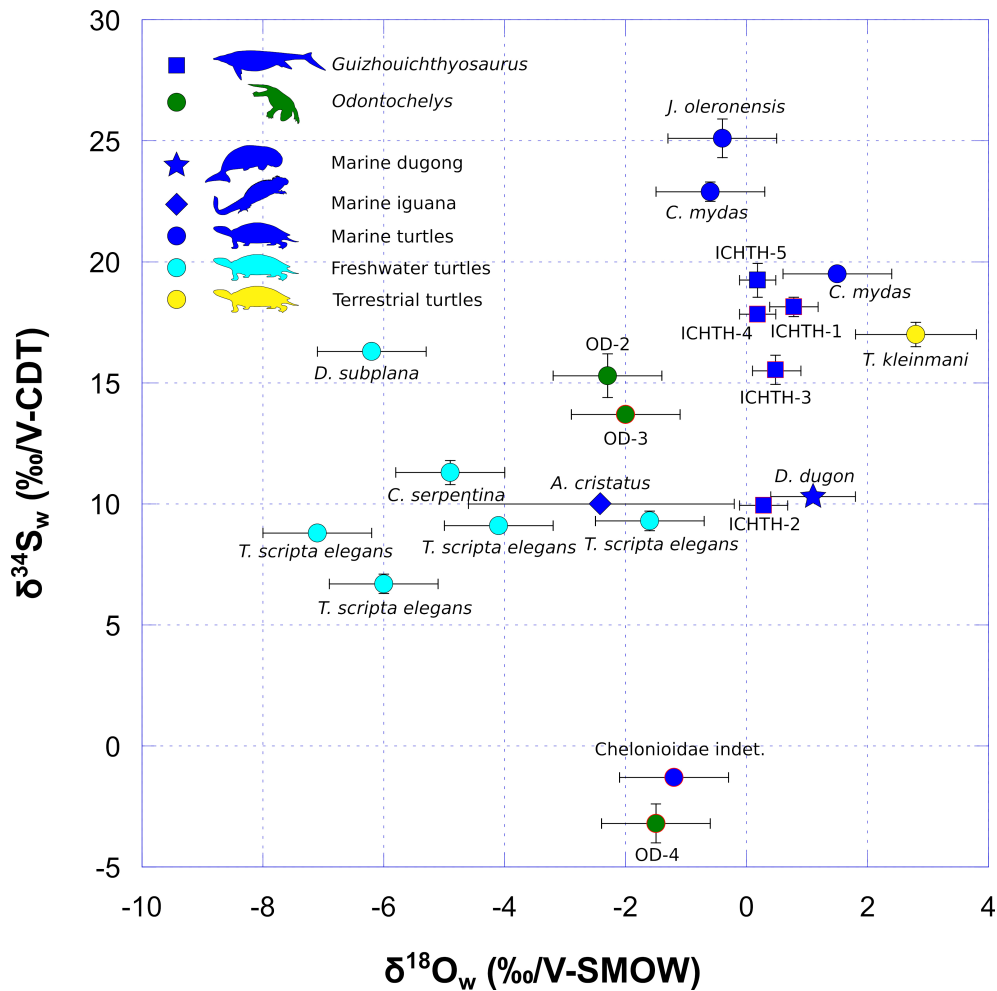
FIGURE 2
Oxygen and sulfur isotope compositions of environmental water ($\delta^{18}O_w$ and $\delta^{34}S_w$) estimated from the $\delta^{18}O_p$ and $\delta^{34}S$ values of vertebrate bioapatites (see Materials and Methods and Supplementary Table 2). $\delta^{18}O_w$ and $\delta^{34}S_w$ values of *Odontochelys* (dark green dots) are compared to the marine carnivorous ichthyosaur *Guizhouichthyosaurus* (dark blue squares), two Mesozoic and two modern marine turtles (dark blue dots), modern freshwater turtle (light blue dots), a modern terrestrial turtle living in a desertic coastal environment (yellow dots), a modern marine iguana (*A. cristatus*; dark blue diamond) and a modern marine dugong (*D. dugon*; dark blue star). Note that the marine iguana and the dugong both have surprisingly low $\delta^{34}S$ values ($\delta^{34}S$ = + 10.0 ‰ and + 10.3 ‰, respectively) according to their marine semi–aquatic and aquatic lifestyles, respectively. One hypothesis to explain such low values is the potential ingestion of substantial volcanic rocky material (in the case of iguana) or sediments (in the case of dugong) containing sulfate minerals relatively depleted (compared to dissolved oceanic sulfates) for the ^{34}S isotopes (e.g., Sakai et al., 1984; Rye, 2005) when the animals graze. Modern values are from Goedert et al. (2018). Data outlined in red correspond to fossil samples whose sulfur isotope composition was modified during diagenesis (see Discussion). Each error bar corresponds to 1 s.d. (Supplementary Table 1).

($\delta^{34}S$ = − 3.2 ‰; S = 1.26 %). Conversely, the Late Jurassic marine turtle *J. oleronensis*, which has the highest $\delta^{34}S$ values ($\delta^{34}S$ = + 25.1 ‰), has a lower sulfur content (0.81 %).

Discussion

Evaluation of primary preservation of stable isotope compositions

After death, bioapatite mineral that composes the skeleton can be modified during diagenesis (e.g., Keenan et al., 2015; Keenan, 2016; Keenan and Engel, 2017). The original content of one or more elements can be altered as well as its pristine isotopic compositions but not in a systematic and *a priori* predictable way, which implies

to evaluate each element separately when assessing diagenesis (e.g., Sponheimer and Lee-Thorp, 2006; Martin et al., 2018).

Here, we used the difference between oxygen isotope compositions of bioapatite phosphate and corresponding structural carbonate ($\delta^{18}O_c$ – $\delta^{18}O_p$), as well as the carbonate content of apatite to evaluate a potential diagenetic alteration of bioapatite carbonate reflected in its carbon and oxygen isotope compositions. Samples that have either $\delta^{18}O_c$ – $\delta^{18}O_p$ differences higher than + 14.7 ‰ or a carbonate content higher than + 13.4 % are considered doubtful regarding a potential diagenetic alteration (Vennemann et al., 2001). Both samples OD-3 and OD-4 have a carbonate content higher than + 13.4 % (Figure 4). Inorganic diagenetic processes may therefore have altered their pristine $\delta^{13}C_c$ and $\delta^{18}O_c$ values (Zazzo et al., 2004). Contrarily, the sample OD-2 has a $\delta^{18}O_c$ – $\delta^{18}O_p$ value and a carbonate content that match expected pristine values (Figure 4).
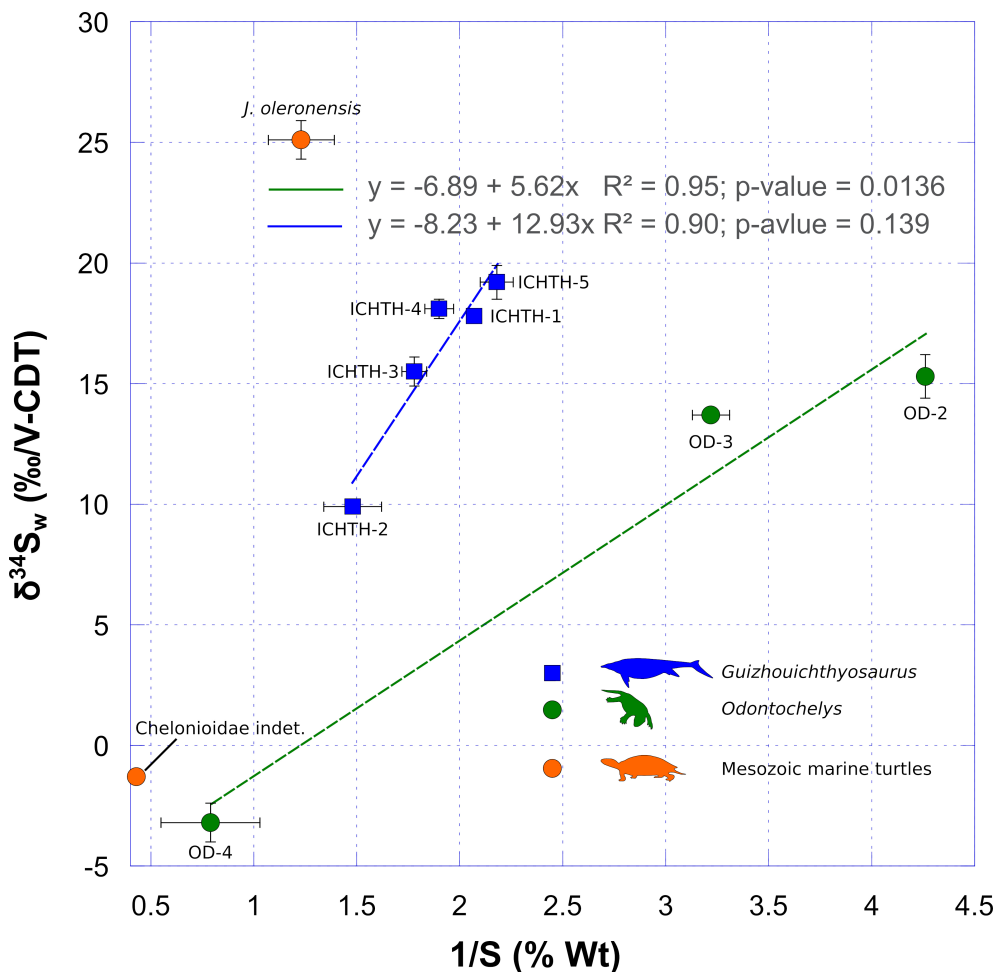
FIGURE 3
Covariation of sulfur isotope composition of bioapatite as a function of the inverse of sulfur content. The increasing sulfur content in fossil bioapatite samples correspond to the probable incorporation of sedimentary sulfide minerals during early diagenesis. Their generally low sulfur isotope compositions tend to lower the sulfur isotope composition measured in fossil bioapatite. Note the similarity between *Odontochelys* OD-4 and Chelonioidea indet. samples. Each error bar corresponds to 1 s.d.

OD-3 has the highest carbonate content (27.0 %), which far exceeds the biological range of apatite-bound carbonate content (Brudevold and Soremark, 1967; Rink and Schwarcz, 1995; Vennemann et al., 2001) and has the highest $\delta^{13}C_c$ and lowest $\delta^{18}O_c$ values for *Odontochelys* samples, which are different from the values of OD-2, representing the same specimen. We consider that the pristine carbon and oxygen isotope compositions of this sample has been overprinted by additional diagenetic carbonate that was not removed by the pretreatment. However, the other specimen (IVPP V 13240) has also a high carbonate content (+ 19.3 %) but its $\delta^{13}C_c$ and $\delta^{18}O_c$ values are coherent with the values of the sample OD-2 representing the other specimen. Thus, OD-2 and OD-4 can be considered as having retained at least a part of their pristine carbon and oxygen isotope compositions. All *Guizhouichthyosaurus* samples have $\delta^{18}O_c$ – $\delta^{18}O_p$ values and carbonate contents that match expected pristine values (Figure 4). We therefore consider that those samples have retained at least a part of their pristine carbon and oxygen isotope compositions.

Contrarily to the oxygen isotope composition of carbonate, the oxygen isotope composition of bioapatite phosphate is more robust

regarding diagenetic alteration (e.g., Shemesh et al., 1983; Lécuyer et al., 1999). Both the specimen of *Odontochelys* IVPP V 15653 and the two specimens of *Guizhouichthyosaurus* have consistent $\delta^{18}O_p$ values. Moreover, the two ichthyosaur individuals have teeth $\delta^{18}O_p$ values higher than associated skull bones ($\delta^{18}O_{p\ tooth}$ − $\delta^{18}O_{p\ skull\ bone}$ = + 0.2 ‰ and + 0.6 ‰ for specimen IVPP V 11865 and IVPP V 11869, respectively), which is coherent with what is observed in modern and fossil cetaceans (Barrick et al., 1992; Amiot et al., 2008; Séon et al., 2022). This result could potentially reflect regional heterothermy in ichthyosaurs as observed in extant cetaceans (Séon et al., 2022). It is therefore an argument in favor of a partial or full preservation of the pristine oxygen isotope composition of bioapatite phosphate.

Sulfur isotopic composition of sulfate that substitutes to phosphate in bioapatite can be overprinted by the addition of diagenetic mineral such as iron sulfide, which can have a very low sulfur isotope composition (e.g., Nehlich, 2015). Although based on a few samples, we observe a non-significant positive correlation between sulfur isotope composition and the inverse of sulfur content for *Odontochelys* (R^2 = 0.95; *p-value* = 0.1389; n = 3)
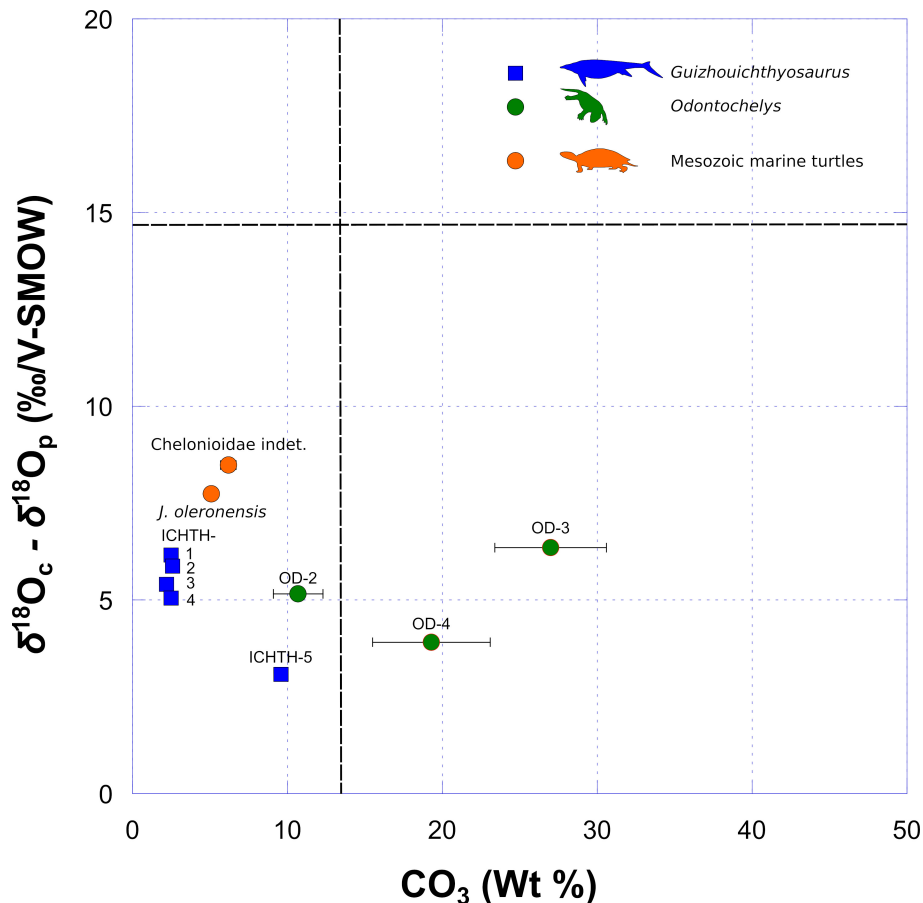
FIGURE 4
Covariation of $\delta^{18}O_p$ and $\delta^{18}O_c$ as a function of carbonate concentration. Samples with both $\delta^{18}O_p - \delta^{18}O_c$ differences higher than + 14.7 ‰ and carbonate contents higher than + 13.4 % are considered to have been potentially affected by diagenetic alteration (see Discussion). Each error bar corresponds to 1 s.d.

and a significant one for *Guizhouichthyosaurus* (R^2 = 0.90; *p-value* = 0.0136; n = 5). This obviously demonstrates that, depending on the sample, a greater or lesser part of the pristine sulfur isotope compositions have been overprinted by the addition of an exogenous source of sulfur having a distinct and lower isotopic composition. This is evident for the sample OD-4, which has the highest sulfur content (1.26 %) of *Odontochelys* samples, associated to the lowest and negative $\delta^{34}S$ value (− 3.2 ‰). This overprinting is also clearly visible for the sample ICHTH-2, which also has the highest sulfur content (0.68 %) of *Guizhouichthyosaurus* samples, also associated to the lowest $\delta^{34}S$ value (+ 9.9 ‰). In the latter case, this is coherent with the accidental incorporation of a fraction of host sediment during the sampling see Method section.

Nonetheless, among *Odontochelys* samples, we assume that the $\delta^{34}S$ values of OD-2 sample, which has the lowest sulfur content (0.23 ± 0.02 %), represents, at least partly, the pristine isotope composition of structural sulfate of apatite. In the same manner, we can consider that ICHTH-5, which has the lowest sulfur content (0.46 ± 0.06 %), represents the pristine isotope composition of structural sulfate of apatite. Assuming these hypotheses, using mass balance equations, we can calculate the sulfur isotope composition

of the diagenetic source of sulfur. For both *Odontochelys* and *Guizhouichthyosaurus*, we calculated consistent and slightly negative $\delta^{34}S$ values for the diagenetic source of sulfur ($\delta^{34}S$ = − 0.05 ± 0.01 ‰ and $\delta^{34}S$ = − 0.17 ± 0.08 ‰). These negative values are compatible with sedimentary sulfides (Nehlich, 2015), such as pyrite, which are commonly precipitated during diagenesis (e.g., Pfretzschner, 2000; Pfretzschner, 2001). We therefore, consider that the samples OD-2 for *Odontochelys* and ICHTH-5 for *Guizhouichthyosaurus* have $\delta^{34}S$ values reflecting those of their structural apatite sulfate, which in turn directly reflects that of the dissolved sulfate in their aquatic environment (Goedert et al., 2018, 2020). All other samples are partially to substantially contaminated and their sulfur isotope compositions cannot be used to draw paleoenvironmental interpretations.

Habitat of *Odontochelys*

Odontochelys was found in black shales, which formed under anoxic conditions at the bottom of a subsiding trough basin (Wang et al., 2008). Early on, it was interpreted as an allochthonous component of the fauna probably originating from marginal areas

of the basin or river deltas (Li et al., 2008). Forelimb proportions were used to support its interpretation as an aquatic taxon (Joyce and Gauthier, 2004; Li et al., 2008). However, *Odontochelys* falls with turtles that inhabit stagnant or small bodies of water primarily due to its greater, primitive phalangeal count (Joyce, 2015). Semi-aquatic turtles are usually characterized by elongated phalanges, while *Odontochelys* has short and robust phalanges resembling those of terrestrial turtles. For Joyce (2015), *Odontochelys* was probably a terrestrial turtle, or, at most, a form living in swampy freshwater environments. However, the description of avascular necrosis on the humerus of the paratype specimen (IVPP V 13240) suggests that *Odontochelys* was indeed an aquatic form (Rothschild and Naples, 2015). Avascular necrosis, a condition arising from decompression syndrome in diving organisms, is common in Cretaceous marine turtles and other Mesozoic marine reptiles, but can also be found in some fossil freshwater turtles (Rothschild, 1987; Martin, 1989; Rothschild, 1991; Motani et al., 1999; Rothschild and Storrs, 2003). Based on the purported presence of a pronounced intertrochanteric fossa, Lichtig and Lucas (2017) concluded that *Odontochelys* was an aquatic form. Finally, using a refined model of forelimb proportion, Dudgeon et al. (2021) also found *Odontochelys* usually associated with aquatic environments, but never with moving or large bodies of water.

Our results show that the $\delta^{18}O_P$ values of both *Odontochelys* and *Guizhouichthyosaurus* are high. We use the phosphate – water isotope fractionation equation established for extant turtles (Barrick et al., 1992; modified by Pouech et al., 2014) and cetaceans (Ciner et al., 2016), considered as a comparable analogue to ichthyosaurs in terms of thermophysiology (Bernard et al., 2010) to estimate the oxygen isotope composition of environmental water ($\delta^{18}O_w$) of *Odontochelys* and *Guizhouichthyosaurus*, respectively (Supplementary Table 2). Calculated $\delta^{18}O_w$ values for *Odontochelys* (− 1.9 ‰ ± 0.4 ‰) are significantly lower (Mann-Whitney U: p-$value$ = 0.035) than those calculated for *Guizhouichthyosaurus* (+ 0.6 ‰ ± 0.3 ‰). When compared to the aquatic vertebrate *Guizhouichthyosaurus* these lower values are consistent with at least a semi-aquatic lifestyle for *Odontochelys* and rules out the hypothesis that *Odontochelys* was terrestrial. Furthermore, coeval conodonts, which are typical marine organisms, yield $\delta^{18}O_P$ values of + 20 ‰ to + 23 ‰ during the Carnian in the North Western Tethys (Hornung et al., 2007). Therefore, the slightly lower $\delta^{18}O_P$ and calculated $\delta^{18}O_w$ values of *Odontochelys* indicate potential freshwater influences in its living aquatic environment and are compatible with a habitat in the coastal zone. This is also supported by comparison with modern sea turtles, which give higher $\delta^{18}O_w$ values (Figure 2). The sulfur isotope composition of dissolved environmental sulfate is recorded without any significant fractionation in bioapatite (Goedert et al., 2018). During the Lower Carnian, $\delta^{34}S$ values of dissolved marine sulfate have been estimated from evaporites of Northern Switzerland with a mean value close to + 16 to + 17 ‰ and assumed to represent that of the global dissolved marine sulfate (Bernasconi et al., 2017). Although they did not measure $\delta^{34}S$ values for the Carnian, Chen and Chu (1988) observed similar trends and values for the Early and Middle Triassic of China and measured $\delta^{34}S$ values around + 16 ‰ for the Late Anisian. If we consider the

samples OD-2 and ICHTH-5 to be the most representative of the sulfur isotope composition of dissolved environmental sulfate, then the higher value of ICHTH-5 (+ 19.2 ± 0.7 ‰) compared to that of OD-2 (+ 15.3 ± 0.9 ‰) is indicative of an offshore marine habitat for *Guizhouichthyosaurus* and a coastal habitat for *Odontochelys*, which is consistent with their respective $\delta^{18}O_P$ values.

The oxygen and sulfur isotope compositions presented herein therefore clearly indicates that *Odontochelys* was an inhabitant of coastal areas. Retrospectively, this conclusion is consistent with the rarity of *Odontochelys* specimens in the sediments of the lower member of the Xiaowa Formation compared to other taxa such as *Guizhouichthyosaurus* and more stenohaline organisms such as ammonoids, crinoids and conodonts (Wang et al., 2008). This indicates that the specimens of *Odontochelys* were transported before their burial in the sediments corresponding to the lower member of the Xiaowa Formation. It is worth to note that spectacular driftwood colonized by the crinoids *Traumatocrinus* have been collected in the same sediments (Wang et al., 2008), which indubitably indicates the presence of allochthonous elements (wood and other plant remains) that have been transported over long distances before their burial. It would now be particularly interesting to reproduce the present study on *Eorhynchochelys sinensis*, which is found in the same locality and a few meters below the horizon of *Odontochelys semitestacea* (Li et al., 2018). *Eorhynchochelys* is based on a unique specimen that lacks obvious morphological adaptations to aquatic environments.

Diet of *Odontochelys*

The two samples OD-2 and OD-4 have clearly different $\delta^{13}C_c$ values than those measured for *Guizhouichthyosaurus* and other turtles, except *Chelonia mydas* (Figure 1). Clementz and Koch (2001) demonstrated that, at the first order, the carbon isotope composition of apatite allows distinguishing foraging zones, although the signal of primary producers can be complicated by trophic level differences, taxon-specific differences in metabolism and differences in the timing of formation and eruption of teeth. Notably, in marine ecosystems, primary producers show strong spatial gradients in $\delta^{13}C$ values, which typically increase from offshore to nearshore ecosystems, with highest values reached by kelp or seagrass (− 17 ‰ to − 11 ‰) in nearshore ecosystems (Clementz and Koch, 2001; Clementz et al., 2007). Freshwater aquatic vegetation has a mean $\delta^{13}C_c$ value around − 27 ‰ today, which is clearly lower than that of nearshore macrophytic marine vegetation (Clementz and Koch, 2001; Clementz et al., 2007). Such high and positive $\delta^{13}C_c$ values measured for *Odontochelys* are rather unique among vertebrates and clearly reflect a foraging zone with a primary source of carbon with elevated $\delta^{13}C$ values. Similarly elevated and positive $\delta^{13}C_c$ values have been documented for the extant green turtle *Chelonia mydas* whose adults consume primarily seagrass and algae, whereas the carnivorous deep-diving leatherback (*Dermochelys coriacea*), olive ridley (*Lepidochelys olivacea*) and loggerhead (*Caretta caretta*) sea turtles have clearly distinct values (Biasatti, 2004; Wheatley et al., 2012; Figure 1). It is also relevant to note that the dugong (*Dugong dugon*), which

predominantly grazes on seagrasses (and also algae) in coastal zone also has elevated, in average positive, $\delta^{13}C_c$ values (MacFadden et al., 2004; Newsome et al., 2010; mean $\delta^{13}C_c$ = + 1.2 ± 0.9 ‰; n = 9 in MacFadden et al., 2004) and that some fossil representatives of the Dugongidae and Protosirenidae also have such elevated $\delta^{13}C_c$ values (MacFadden et al., 2004; Clementz et al., 2006; Newsome et al., 2010). Thus, we interpret the positive and high $\delta^{13}C_c$ values measured for *Odontochelys* ($\delta^{13}C_c$ = + 0.50 ‰ ± 0.54; n = 2) as the result of an herbivorous feeding ecology in the nearshore marine zone (Figure 1). Assuming an herbivorous diet, the $\delta^{13}C$ value of the food would be around − 11.5 ‰ according to an isotopic fractionation of + 12 ‰ between the diet and bioapatite of extant herbivorous turtles (Biasatti, 2004). This value of − 11.5 ‰ is coherent with that measured for present-day macrophytic nearshore ecosystem (Clementz and Koch, 2001).

The present results therefore lead to the interpretation of *Odontochelys* as a nearshore herbivorous forager feeding on marine macrophytes, which would during the Triassic consists mostly of algae. It is interesting here to draw a parallel with the extant marine iguana, *Amblyrhynchus cristatus*, which also feeds exclusively on algae (Vitousek et al., 2007) and which can also record high $\delta^{13}C_c$ values up to − 0.3 ‰ for individuals that predominantly feed on kelp (Wheatley et al., 2012; Figure 1). Marine iguanas have powerful limbs (especially the forelimbs) with strong claws that they use to cling to the rock on which their food grows and to climb out of the water to bask and rest. They actually spend most of their time out of the water. Juveniles and females usually feed in the intertidal zone during low tide, using their claws to prevent being swept away by waves. Larger males tend to feed offshore, diving to reach underwater rocks on which they cling with their strong claws while feeding on algae (Trillmich, 1979; Trillmich and Trillmich, 1986; Wikelski and Trillmich, 1994). The relatively short and robust forelimbs with stout proximal phalanges and strong claws of *Odontochelys* were probably poorly suited for efficient swimming (Joyce, 2015; Schoch et al., 2019). However, they could be used by the animal to cling to rocks while feeding on algae underwater, like for the marine iguana. It has also been proposed that the completion of the plastron in *Odontochelys* appeared as an adaption for swimming to serve as ballast (Rieppel, 2017; Lyson and Bever, 2020). If *Odontochelys* is indeed an ecological analogue of the marine iguana, then the extra weight of the fully formed plastron would surely help the animal to dive and reach its food underwater.

The diet of other early stem turtles is poorly documented. The marginal and palatal teeth of *Eunotosaurus*, *Pappochelys*, *Eorhynchochelys*, and *Odontochelys* are small and unspecialized (Li et al., 2008; Bever et al., 2015; Schoch and Sues, 2015; Li et al., 2018). More derived stem turtles with a fully formed shell (Testudinata) such as *Proganochelys quenstedti* and *Australochelys africanus* lack marginal teeth. Instead, they have an edentulous beak with narrow triturating surfaces that reveal nothing of their diet (Gaffney, 1990; Gaffney and Kitching, 1995). The presence of scratches and pits on the palatal teeth of *Proganochelys* may suggest an herbivorous diet (Xafis et al., 2018), but these results

have not yet been formally published. Finally, coprolites that are tentatively assigned to *Proterochersis porebensis* would suggest an omnivorous diet (fish and plants) for this species (Bajdek et al., 2019). Many modern turtles have a feeding strategy that can be qualified as omnivorous and opportunistic (Pritchard, 1979; Ernst and Barbour, 1989). This might also have been the case of early stem turtles, although it is impossible at the moment to draw firm conclusions based on the evidence at our disposal. In contrast, some modern turtles are characterized by more specialized diets. For example, the leatherback sea turtle (*Dermochelys coriacea*) feeds preferentially on jellyfish, while durophagy (feeding on hard-shelled organisms) evolved repeatedly in several groups of turtles (Ernst and Barbour, 1989; Claude et al., 2004). In this context, the present study represents the earliest case of diet specialization in *Pan-Testudines*. However, further research is needed to investigate if herbivory was more widespread among stem turtles or even ancestral for turtles.

Conclusion

Although based on a small number of available samples, multi-stable isotope compositions of bioapatite yield consistent results allowing us to confidently reconstruct the paleoecology of the earliest stem turtle with a complete plastron. Oxygen and sulfur isotope compositions clearly demonstrate that *Odontochelys* lived in a coastal marine environment submitted to some freshwater influence. Hence, it seems reasonable to consider that the typical turtle plastron indeed evolved in an aquatic context. *Odontochelys* is also characterized by an unusual carbon isotope composition indicating that it was feeding primarily on marine macrophytes. Such an unusual isotopic signature is uncommon in vertebrates but can be found in the green sea turtle (*Chelonia mydas*) and the dugong (*Dugong dugon*), which both feed mostly on algae and seagrass, and the marine iguana (*Amblyrhynchus cristatus*), which feeds exclusively on algae. Given the forelimb morphology of *Odontochelys*, which is poorly adapted to efficient swimming, it is relevant to draw a parallel with the marine iguana that uses its strong limbs and claws to cling to rock while feeding on algae underwater. Therefore, the first incursion of *Pan-Testudines* (turtles + their stem) into marine environments appears to be one into a very specialized ecological niche.

Materials and methods

Samples

Odontochelys semitestacea is known from only three specimens hosted at the Institute of Vertebrate Paleontology and Paleoanthropology (IVPP) of the Chinese Academy of Sciences, Beijing, China (Li et al., 2008): the holotype specimen (IVPP V 15639), which consists of a complete articulated skeleton; the paratype specimen (IVPP V 13240), which consists of a second

complete articulated skeleton, only prepared in the ventral view; and a referred specimen (IVPP V 15653), which consists of a partial disarticulated skeleton. We had the opportunity to sample and analyze the paratype and the referred specimen. We also analyzed the stable isotope compositions of two ichthyosaur specimens (IVPP V 11865 and IVPP V 11869), coming from the same sediments. They were first described by Li and You (2002) and later referred to the taxon *Shastasaurus tangae* (Shang and Li, 2009) according to their close affinity with the North American taxon *Shastasaurus* spp. They are now considered to belong to the distinct genus *Guizhouichthyosaurus tangae* (Ji et al., 2016).

For each specimen, around 50 mg of bioapatite powder was collected using a spherical diamond-tipped drill bit in order to perform the carbon and oxygen isotope analyses of carbonate (10 mg), the oxygen isotope analysis of phosphate (3 mg), and the sulfur isotope analysis (20 mg) of bioapatite.

We collected one bioapatite sample (OD-2) for the paratype specimen and two bioapatite samples (OD-3 and OD-4) for the referred specimen of *Odontochelys* (Supplementary Table 1). We also collected the sediment associated with the referred specimen (OD-1). For the *Guizhouichthyosaurus* specimen IVPP V 11865 we collected three bioapatite samples (ICHTH-1:3) corresponding to one bone and two teeth and for the *Guizhouichthyosaurus* specimen IVPP V 11869 we collected two bioapatite samples (ICHTH-4 and ICHTH-5) corresponding to one bone and one tooth (Supplementary Table 1). During the sampling of ICHTH-2 we noticed that a fraction of surrounding sediments was potentially sampled with the tooth (cf. results).

Finally, in order to replace our results in the context of the turtle clade, we also compared the stable isotopic data obtained for *Odontochelys* to that of two Mesozoic marine turtles. We sampled a skull bone from a *Jurassichelon oleronensis* specimen from the Upper Kimmeridgian of Chassiron (specimen deposited in the Museum Dinoléron) and an osteocyte fragment from a marine turtle (Chelonioidea indet.) from the Middle Campanian of the Talmont cliffs (Supplementary Table 1). We also compared the stable isotopic data obtained for *Odontochelys* to that of several modern species of known ecology (obtained from the literature; Supplementary Table 1).

Carbon and oxygen isotope analyses of bioapatite carbonate

Each 10 mg aliquot of bioapatite powder was pre-treated according to the protocol described by (Koch et al., 1997). For each sample, bioapatite powder was washed with a 3.5 % NaOCl solution to remove possible organic matter, followed by a 0.1 M acetic acid solution to remove diagenetic carbonates. The volume of solution/mass of powder ratio was held constant at 25 µl.mg^{-1} for both treatments. Each treatment lasted for 24 h, and samples were rinsed 5 times with double-deionized water. Carbon and oxygen isotope measurements of bioapatite carbonates were performed at

the Laboratoire d'Ecologie des Hydrosystèmes Naturels et Anthropisés (LEHNA; UMR CNRS 5023), part of the national RéGEF network in Lyon. The system used was an an isoFLOW automated preparation device connected on line in continuous flow mode to a precisION mass spectrometer operated by ionOS software from Elementar Uk Ltd. Sample powders were loaded in round-bottomed, non-evacuated LABCO Exetainer® 3.7 ml soda glass vials. For each pre-treated sample, three aliquots of approximately 2 mg each were reacted with anhydrous oversaturated phosphoric acid prepared according to the protocol described by McCrea (1950). The reaction took place at 70 °C in a temperature regulated sample tray. The CO_2 gas generated during the acid digestion of the carbonate sample was then transferred to the mass spectrometer *via* a centrION interface. A calibrated CO_2 gas was used as a monitoring gas. Carrara Marble ($\delta^{18}O$ = − 1.841 ‰ VPDB; $\delta^{13}C$ = + 2.025 ‰ VPDB; Fourel et al., 2016) and NBS18 ($\delta^{18}O$ = − 23.2 ‰ VPDB; $\delta^{13}C$ = − 5.014 ‰ VPDB; Friedman et al., 1982; Hut, 1987; Coplen et al., 2006) were used as calibration materials. The normalization incorporates the CO_2-carbonate acid fractionation factor for calcite. Additionally, aliquots of NBS120c (Natural Miocene phosphorite from Florida), a standard of chemical composition close to bioapatite, were placed at the beginning of each analytical batch to check that analytical conditions were suitable to analyze bioapatite samples. Four aliquots of Carrara Marble were placed at the beginning and at the end of each analytical batch to correct for the instrumental drift over time. No significant drift was recorded during experiments (Mann-Whitney pairwise: *p-value* = 0.3778 and *p-value* = 0.5614 for three series of (n = 4) Carrara Marble). Aliquots of Carrara Marble of different weights (200 µg to 800 µg) were measured in order to estimate the carbonate content of bioapatite samples based on the peak height of CO_2 detected by the mass spectrometer. External reproducibility (2σ) was lower than ± 0.1 ‰ for $\delta^{13}C_c$ and ± 0.2 ‰ for $\delta^{18}O_c$ during the analytical session. Data are reported as $\delta^{13}C_c$ and $\delta^{18}O_c$ values in ‰ versus VPDB. (Figure 1; Supplementary Table 1). $\delta^{18}O_c$ values are also reported versus V-SMOW (e.g., Supplementary Table 1), using the equation of Coplen et al. (1983) (see also Brand et al., 2014; Kim et al., 2015).

Oxygen isotope analysis of bioapatite phosphate

Each 3 mg aliquot of bone powder was treated according to the wet chemistry protocol initially described by Crowson et al. (1991), and subsequently modified by Lécuyer et al. (1993) and then adapted by Bernard et al. (2009) for small sample weights (3 mg). This protocol involves the isolation of phosphate ions (PO_4^{3-}) from bioapatite as silver phosphate (Ag_3PO_4) crystals using acid dissolution and anion-exchange resin. For each sample, enamel powder was dissolved in 1 ml of 2 M HF overnight. The CaF_2 residue was separated in a centrifuge and the solution neutralized by adding 1 ml of 2 M KOH. Amberlite anion-exchange resin (1.5 ml)

was added to the solution to separate the PO_4^{3-} ions. After 4 h, the solution was removed and the resin was eluted with 6 ml of 0.5 M NH_4NO_3. After 4 h, 0.1 ml of NH_4OH and 3 ml of an ammoniacal solution of $AgNO_3$ were added and the samples were placed in a thermostatic bath at 70 °C for 6 h, enabling the precipitation of Ag_3PO_4 crystals. Oxygen isotope compositions were measured using a high-temperature pyrolysis technique involving a VarioPYROcube elemental analyser using purge and trap technology for gas separation, connected in continuous flow mode to an Isoprime isotopic ratio mass spectrometer (the EA-Py-CF-IRMS technique; Lécuyer et al., 2007; Fourel et al., 2011). For each sample, 5 aliquots of 300 μg of Ag_3PO_4 were mixed with 300 μg of pure graphite powder and loaded in silver foil capsules. Pyrolysis was performed at 1450 °C. Measurements were calibrated against NBS120c ($\delta^{18}O$ = + 21.7 ‰ V-SMOW; Lécuyer et al., 1993) and NBS 127 (barium sulfate, $BaSO_4$: $\delta^{18}O$ = + 9.30 ‰ V-SMOW; Hut, 1987; Halas and Szaran, 2001). Silver phosphate samples precipitated from standard NBS 120c were repeatedly analyzed ($\delta^{18}O$ = 21.8 ‰; 1σ = 0.3 ‰; n = 8) along with the silver phosphate samples derived from fossil bioapatites to ensure that no isotopic fractionation took place during the wet chemistry. The sample average standard deviation was 0.3 ± 0.13 ‰ for $\delta^{18}O_p$ measurements. Data are reported as $\delta^{18}O_p$ values in ‰ versus V-SMOW (Supplementary Table 1).

Sulfur isotope analysis of bioapatite

Sulfur isotope compositions were measured at the Laboratoire d'Ecologie des Hydrosystèmes Naturels et Anthropisés (LEHNA; UMR CNRS 5023) using a VarioPYROcube^{TM} elemental analyser in NCS combustion mode interfaced in continuous-flow mode with an Isoprime100^{TM} isotope ratio mass spectrometer. For each bone apatite sample, 3 aliquots of 7 mg of bioapatite powder were mixed with 20 mg of pure tungsten oxide (WO3) powder and loaded in tin foil capsules. Tungsten oxide is a powerful oxidant ensuring the full thermal decomposition of apatite sulfate into sulfur dioxide (SO_2) gas (Goedert et al., 2016). Measurements have been calibrated against the NBS 127 (barium sulfate, $BaSO_4$ $\delta^{34}S$ = + 20.3 ‰ V-CDT; Halas and Szaran, 2001) and S1 (silver sulfide, Ag_2S $\delta^{34}S$ = − 0.3 ‰ V-CDT; Robinson, 1995) international standards. For each analytical run of bone samples, we have also analysed BCR32 samples (S % = 0.72, certified value (Community Bureau of Reference, 1982); $\delta^{34}S$ = + 18.4 ‰ V-CDT (Fourel et al., 2015; Goedert et al., 2016)) as a compositional (S % = 0.81 ± 0.1 %) and isotopic standard ($\delta^{34}S$ = + 18.3 ± 0.1 ‰ V-CDT) to ensure that analytical conditions were optimal to perform sulfur isotope analyses of samples with low-S content. The sample average standard deviation for $\delta^{34}S$ measurements is 0.5 ‰ ± 0.3 ‰ (s.e.m). Data are reported as $\delta^{34}S$ in ‰ versus V-CDT (Supplementary Table 1).

Stable isotope composition of environmental water

Oxygen isotope composition of environmental water ($\delta^{18}O_w$) was calculated from measured $\delta^{18}O_p$ values using published $\delta^{18}O_p$ − $\delta^{18}O_w$ fractionation equations (Figure 2; Supplementary Table 2). Previous works demonstrated that the sulfur isotope compositions of environmental waters ($\delta^{34}S_w$) are recorded in bioapatite tissues with minute isotopic fractionation (Goedert et al., 2018). We thus considered here that measured $\delta^{34}S$ values of bioapatite directly reflects $\delta^{34}S_w$ values (Figure 2).

Statistical treatment

Since normality and homoscedasticity of the isotopic data were not validated, the non-parametric Mann-Whitney-Wilcoxon test was used to compare median values between two or more observational series, respectively. Tests were performed using Past 4.03. The level of significance for statistical analyses was set at a *p-value* < 0.05.

Data availability statement

The original contributions presented in the study are included in the article/Supplementary Material. Further inquiries can be directed to the corresponding author.

Author contributions

JG, RA and CLé conceived the project. RB, GB, and CLi provided access and helped to sample the material. JG and RA sampled the material. JG performed chemical preparation of the material prior to stable isotopic measurements. JG, FF, LS, and RA performed stable isotopic analyses. JG and JA wrote the first version of the manuscript. All authors contributed to the article and approved the submitted version.

Funding

Acknowledgments

Conflict of interest

The authors declare that the research was conducted in the absence of any commercial or financial relationships that could be construed as a potential conflict of interest.

Publisher's note

All claims expressed in this article are solely those of the authors and do not necessarily represent those of their affiliated organizations, or those of the publisher, the editors and the reviewers. Any product that may be evaluated in this article, or claim that may be made by its manufacturer, is not guaranteed or endorsed by the publisher.

Supplementary material

The Supplementary Material for this article can be found online at: https://www.frontiersin.org/articles/10.3389/fevo.2023.1175128/full#supplementary-material

References

Amiot, R., Göhlich, U. B., Lécuyer, C., de Muizon, C., Cappetta, H., Fourel, F., et al. (2008). Oxygen isotope compositions of phosphate from Middle Miocene–Early Pliocene marine vertebrates of Peru. *Palaeogeogr. Palaeoclimatol. Palaeoecol.* 264, 85–92. doi: 10.1016/j.palaeo.2008.04.001

Bajdek, P., Szczygielski, T., Kapuścińska, A., and Sulej, T. (2019). Bromalites from a turtle-dominated fossil assemblage from the Triassic of Poland. *Palaeogeogr. Palaeoclimatol. Palaeoecol.* 520, 214–228. doi: 10.1016/j.palaeo.2019.02.002

Barrick, R. E., Fischer, A. G., Kolodny, Y., Luz, B., and Bohaska, D. (1992). Cetacean bone oxygen isotopes as proxies for Miocene ocean composition and glaciation. *Palaios*, 521–531. doi: 10.2307/3514849

Bernard, A., Daux, V., Lécuyer, C., Brugal, J.-P., Genty, D., Wainer, K., et al. (2009). Pleistocene seasonal temperature variations recorded in the δ18O of Bison priscus teeth. *Earth Planet. Sci. Lett.* 283, 133–143. doi: 10.1016/j.epsl.2009.04.005

Bernard, A., Lécuyer, C., Vincent, P., Amiot, R., Bardet, N., Buffetaut, E., et al. (2010). Regulation of body temperature by some Mesozoic marine reptiles. *Science* 328, 1379–1382. doi: 10.1126/science.1187443

Bernasconi, S. M., Meier, I., Wohlwend, S., Brack, P., Hochuli, P. A., Bläsi, H., et al. (2017). An evaporite-based high-resolution sulfur isotope record of Late Permian and Triassic seawater sulfate. *Geochim. Cosmochim. Acta* 204, 331–349. doi: 10.1016/j.gca.2017.01.047

Bever, G. S., Lyson, T. R., Field, D. J., and Bhullar, B.-A. S. (2015). Evolutionary origin of the turtle skull. *Nature* 525, 239–242. doi: 10.1038/nature14900

Bever, G. S., Lyson, T. R., Field, D. J., and Bhullar, B.-A. S. (2016). The amniote temporal roof and the diapsid origin of the turtle skull. *Zoology* 119, 471–473. doi: 10.1016/j.zool.2016.04.005

Biasatti, D. M. (2004). Stable carbon isotopic profiles of sea turtle humeri: implications for ecology and physiology. *Palaeogeogr. Palaeoclimatol. Palaeoecol.* 206, 203–216. doi: 10.1016/j.palaeo.2004.01.004

Brand, W. A., Coplen, T. B., Vogl, J., Rosner, M., and Prohaska, T. (2014). Assessment of international reference materials for isotope-ratio analysis (IUPAC Technical Report). *Pure Appl. Chem.* 86, 425–467. doi: 10.1515/pac-2013-1023

Brudevold, F., and Soremark, R. (1967). Chemistry of the mineral phase of enamel. *Struct. Chem. Organ. teeth* 2, 247–277.

Chen, J.-S., and Chu, X.-L. (1988). Sulfur isotope composition of Triassic marine sulfates of South China. *Chem. Geol.: Isotope Geosci. Sec.* 72, 155–161.

Ciner, B., Wang, Y., and Parker, W. (2016). Oxygen isotopic variations in modern cetacean teeth and bones: implications for ecological, paleoecological, and paleoclimatic studies. *Sci. Bull.* 61 (1), 92–104. doi: 10.1007/s11434-015-0921-x

Claude, J., Pritchard, P., Tong, H., Paradis, E., and Auffray, J.-C. (2004). Ecological correlates and evolutionary divergence in the skull of turtles: A geometric morphometric assessment. *Sys. Biol.* 53, 937–952. doi: 10.1080/10635150490889498

Clementz, M. T., Goswami, A., Gingerich, P. D., and Koch, P. L. (2006). Isotopic records from early whales and sea cows: contrasting patterns of ecological transition. *J. Vertebrate Paleontol.* 26, 355–370. doi: 10.1671/0272-4634(2006)26[355:IRFEWA]2.0.CO;2

Clementz, M. T., and Koch, P. L. (2001). Differentiating aquatic mammal habitat and foraging ecology with stable isotopes in tooth enamel. *Oecologia* 129, 461–472. doi: 10.1007/s004420100745

Clementz, M. T., Koch, P. L., and Beck, C. A. (2007). Diet induced differences in carbon isotope fractionation between sirenians and terrestrial ungulates. *Mar. Biol.* 151, 1773–1784. doi: 10.1007/s00227-007-0616-1

Community Bureau of Reference (1982). *Certified reference material certificate of analyses for BCR No. 32. Commission of the European Communities, Report No. 541.*

Coplen, T. B., Brand, W. A., Gehre, M., Gröning, M., Meijer, H. A. J., Toman, B., et al. (2006). New guidelines for δ13C measurements. *Anal. Chem.* 78, 2439–2441. doi: 10.1021/ac052027c

Coplen, T. B., Kendall, C., and Hopple, J. (1983). Comparison of stable isotope reference samples. *Nature* 302, 236–238. doi: 10.1038/302236a0

Crowson, R. A., Showers, W. J., Wright, E. K., and Hoering, T. C. (1991). Preparation of phosphate samples for oxygen isotope analysis. *Anal. Chem.* 63, 2397–2400. doi: 10.1021/ac00020a038

deBraga, M., and Rieppel, O. (1997). Reptile phylogeny and the interrelationships of turtles. *Zoological J. Linn. Soc.* 120, 281–354. doi: 10.1111/j.1096-3642.1997.tb01280.x

Dudgeon, T. W., Livius, M. C., Alfonso, N., Tessier, S., and Mallon, J. C. (2021). A new model of forelimb ecomorphology for predicting the ancient habitats of fossil turtles. *Ecol. Evol.* 11, 17071–17079. doi: 10.1002/ece3.8345

Ernst, C. H., and Barbour, R. W. (1989). *Turtles of the World* (Smithonian Institution Press).

Fourel, F., Martineau, F., Lécuyer, C., Kupka, H. J., Lange, L., Ojeimi, C., et al. (2011). 18O/16O ratio measurements of inorganic and organic materials by elemental analysis–pyrolysis–isotope ratio mass spectrometry continuous-flow techniques. *Rapid Commun. Mass Spectrometry* 25, 2691–2696. doi: 10.1002/rcm.5056

Fourel, F., Martineau, F., Seris, M., and Lécuyer, C. (2015). Measurement of 34S/32S ratios of NBS 120c and BCR 32 phosphorites using purge and trap EA-IRMS technology. *Geostand. Geoanal. Res.* 39, 47–53. doi: 10.1111/j.1751-908X.2014.00297.x

Fourel, F., Martineau, F., Tóth, E. E., Görög, A., Escarguel, G., and Lécuyer, C. (2016). Carbon and oxygen isotope variability among foraminifera and ostracod carbonated shells Vol. 70 (Annales Universitatis Mariae Curie-Sklodowska, sectio AAA–Physica), 133.

Friedman, I., O'Neil, J., and Cebula, G. (1982). Two new carbonate stable-isotope standards. *Geostand. Newslett.* 6, 11–12. doi: 10.1111/j.1751-908X.1982.tb00340.x

Gaffney, E. S. (1990). *The comparative osteology of the Triassic turtle Proganochelys.* Vol. 194 (Bulletin of the American Museum of Natural History), 1–263.

Gaffney, E. S., and Kitching, J. W. (1995). The morphology and relationships of *Australochelys*, an Early Jurassic turtle from South Africa. *Am. Museum Novitates* 3130, 1–29.

Gemmell, N. J., Rutherford, K., Prost, S., Tollis, M., Winter, D., Macey, J. R., et al. (2020). The tuatara genome reveals ancient features of amniote evolution. *Nature* 584, 403–409. doi: 10.1038/s41586-020-2561-9

Goedert, J., Amiot, R., Berthet, D., Fourel, F., Simon, L., and Lécuyer, C. (2020). Combined oxygen and sulphur isotope analysis—a new tool to unravel vertebrate (paleo)-ecology. *Sci. Nat.* 107, 1–9. doi: 10.1007/s00114-019-1664-3

Goedert, J., Fourel, F., Amiot, R., Simon, L., and Lécuyer, C. (2016). High-precision 34S/32S measurements in vertebrate bioapatites using purge-and-trap EA-IRMS technology. *Rapid Commun. Mass Spectrometry (À COMPLÉTER)* 30 (18), 2002–2008.

Goedert, J., Lécuyer, C., Amiot, R., Arnaud-Godet, F., Wang, X., Cui, L., et al. (2018). Euryhaline ecology of early tetrapods revealed by stable isotopes. *Nature* 558, 68–72. doi: 10.1038/s41586-018-0159-2

Halas, S., and Szaran, J. (2001). Improved thermal decomposition of sulfates to SO2 and mass spectrometric determination of δ34S of IAEA SO-5, IAEA SO-6 and NBS-127 sulfate standards. *Rapid Commun. Mass Spectrom* 15, 1618–1620. doi: 10.1002/rcm.416

Hornung, T., Brandner, R., Krystyn, L., Joachimski, M. M., and Keim, L. (2007). Multistratigraphic constraints on the NW Tethyan "Carnian crisis". *Global Triassic* 41, 59–67.

Hut, G. (1987). "Stable isotope reference samples for geochemical and hydrological investigations," in *Consultant Group Meeting IAEA, Vienna, 16–18 September 1985, Report to the Director General*, vol. 42. (Vienna: International Atomic Energy Agency).

Ji, C., Jiang, D.-Y., Motani, R., Rieppel, O., Hao, W. C., Sun, Z. Y., et al. (2016). Phylogeny of the Ichthyopterygia incorporating recent discoveries from South China. *J. Vertebrate Paleontol.* 36, e1025956. doi: 10.1080/02724634.2015.1025956

Joyce, W. G. (2015). The origin of turtles: a paleontological perspective. *J. Exp. Zool. Part B: Mol. Dev. Evol.* 324, 181–193. doi: 10.1002/jez.b.22609

Joyce, W. G., and Gauthier, J. A. (2004). Palaeoecology of Triassic stem turtles sheds new light on turtle origins. *Proc. R. Soc. London Ser. B: Biol. Sci.* 271, 1–5. doi: 10.1098/rspb.2003.2523

Keenan, S. W. (2016). From bone to fossil: A review of the diagenesis of bioapatite. *Am. Mineralogist* 101, 1943–1951. doi: 10.2138/am-2016-5737

Keenan, S. W., and Engel, A. S. (2017). Early diagenesis and recrystallization of bone. *Geochim. Cosmochim. Acta* 196, 209–223. doi: 10.1016/j.gca.2016.09.033

Keenan, S. W., Engel, A. S., Roy, A., and Bovenkamp-Langlois, G. L. (2015). Evaluating the consequences of diagenesis and fossilization on bioapatite lattice structure and composition. *Chem. Geol.* 413, 18–27. doi: 10.1016/j.chemgeo.2015.08.005

Kim, S.-T., Coplen, T. B., and Horita, J. (2015). Normalization of stable isotope data for carbonate minerals: Implementation of IUPAC guidelines. *Geochim. cosmochim. Acta* 158, 276–289. doi: 10.1016/j.gca.2015.02.011

Koch, P. L., Tuross, N., and Fogel, M. L. (1997). The effects of sample treatment and diagenesis on the isotopic integrity of carbonate in biogenic hydroxylapatite. *J. Archaeological Sci.* 24, 417–429. doi: 10.1006/jasc.1996.0126

Laurin, M., and Reisz, R. R. (1995). A reevaluation of early amniote phylogeny. *Zoological J. Linn. Soc.* 113, 165–223. doi: 10.1111/j.1096-3642.1995.tb00932.x

Lécuyer, C., Fourel, F., Martineau, F., Amiot, R., Bernard, A., Daux, V., et al. (2007). High-precision determination of $^{18}O/^{16}O$ ratios of silver phosphate by EA-pyrolysis-IRMS continuous flow technique. *J. Mass Spectrometry* 42, 36–41. doi: 10.1002/jms.1130

Lécuyer, C., Grandjean, P., O'Neil, J. R., Cappetta, H., and Martineau, F. (1993). Thermal excursions in the ocean at the Cretaceous—Tertiary boundary (northern Morocco): δ^{18}O record of phosphatic fish debris. *Palaeogeogr. Palaeoclimatol. Palaeoecol.* 105, 235–243. doi: 10.1016/0031-0182(93)90085-W

Lécuyer, C., Grandjean, P., and Sheppard, S. M. F. (1999). Oxygen isotope exchange between dissolved phosphate and water at temperatures ≤135°C: inorganic versus biological fractionations. *Geochim. Cosmochim. Acta* 63, 855–862. doi: 10.1016/S0016-7037(99)00096-4

Lee, M. S. (1997). Pareiasaur phylogeny and the origin of turtles. *Zoological J. Linn. Soc.* 120, 197–280. doi: 10.1111/j.1096-3642.1997.tb01279.x

Lee, M. S. Y. (2013). Turtle origins: insights from phylogenetic retrofitting and molecular scaffolds. *J. Evolutionary Biol.* 26, 2729–2738. doi: 10.1111/jeb.12268

Li, C., Fraser, N. C., Rieppel, O., and Wu, X.-C. (2018). A Triassic stem turtle with an edentulous beak. *Nature* 560, 476–479. doi: 10.1038/s41586-018-0419-1

Li, C., Wu, X.-C., Rieppel, O., Wang, L. T., and Zhao, L. J. (2008). An ancestral turtle from the Late Triassic of southwestern China. *Nature* 456, 497–501. doi: 10.1038/nature07533

Li, C., and You, H. (2002). *Cymbospondylus* from the upper triassic of Guizhou, China. [Ku chi Chui Tung wu yu ku jen Lei]: *Vertebrata Palasiatica* 40, 9–16.

Lichtig, A. J., and Lucas, S. G. (2017). A simple method for inferring habitats of extinct turtles. *Palaeoworld* 26, 581–588. doi: 10.1016/j.palwor.2017.02.001

Lichtig, A. J., and Lucas, S. G. (2021). *Chinlechelys* from the Upper Triassic of New Mexico, USA, and the origin of turtles. *Palaeontologia Electronica* 24, a–13. doi: 10.26879/886

Lyson, T. R., and Bever, G. S. (2020). Origin and evolution of the turtle body plan. Annual Review of Ecology. *Evolution Syst.* 51. doi: 10.1146/annurev-ecolsys-110218-024746

Lyson, T. R., Bever, G. S., Bhullar, B.-A. S., Joyce, W. G., and Gauthier, J. A. (2010). Transitional fossils and the origin of turtles. *Biol. Lett.* 6, 830–833. doi: 10.1098/rsbl.2010.0371

Lyson, T. R., Bever, G. S., Scheyer, T. M., Hsiang, A. Y., and Gauthier, J. A. (2013). Evolutionary origin of the turtle shell. *Curr. Biol.* 23, 1113–1119. doi: 10.1016/j.cub.2013.05.003

Lyson, T. R., Rubidge, B. S., Scheyer, T. M., de Queiroz, K., Schachner, E. R., Smith, R. M. H., et al. (2016). Fossorial origin of the turtle shell. *Curr. Biol.* 26, 1887–1894. doi: 10.1016/j.cub.2016.05.020

Lyson, T. R., Schachner, E. R., Botha-Brink, J., Scheyer, T. M., Lambertz, M., Bever, G. S., et al. (2014). Origin of the unique ventilatory apparatus of turtles. *Nat. Commun.* 5, 1–11. doi: 10.1038/ncomms6211

MacFadden, B. J., Higgins, P., Clementz, M. T., and Jones, D. S. (2004). Diets, habitat preferences, and niche differentiation of Cenozoic sirenians from Florida: evidence from stable isotopes. *Paleobiology* 30, 297–324. doi: 10.1666/0094-8373(2004)030<0297:DHPAND>2.0.CO;2

Martin, L. D. (1989). Paleopathology and diving mosasaurs. *Amer Scientist* 77, 460–467.

Martin, J. E., Tacail, T., and Balter, V. (2017). Non-traditional isotope perspectives in vertebrate palaeobiology. *Palaeontology*. doi: 10.1111/pala.12300

Martin, J. E., Tacail, T., Cerling, T. E., and Balter, V. (2018). Calcium isotopes in enamel of modern and Plio-Pleistocene East African mammals. *Earth Planet. Sci. Lett.* 503, 227–235. doi: 10.1016/j.epsl.2018.09.026

McCrea, J. M. (1950). On the isotopic chemistry of carbonates and a paleotemperature scale. *J. Chem. Phys.* 18, 849–857. doi: 10.1063/1.1747785

Motani, R., Rothschild, B. M., and Wahl, W. (1999). Large eyeballs in diving ichthyosaurs. *Nature* 402, 747–747. doi: 10.1038/45435

Nehlich, O. (2015). The application of sulphur isotope analyses in archaeological research: A review. *Earth-Sci. Rev.* 142, 1–17. doi: 10.1016/j.earscirev.2014.12.002

Newsome, S. D., Clementz, M. T., and Koch, P. L. (2010). Using stable isotope biogeochemistry to study marine mammal ecology. *Mar. Mammal Sci.* 26, 509–572. doi: 10.1111/j.1748-7692.2009.00354.x

Pfretzschner, H.-U. (2000). Pyrite formation in Pleistocene bones-a case of very early mineral formation during diagenesis. *Neues Jahrbuch für Geologie und Paläontologie-Abhandlungen*, 143–160. doi: 10.1127/njgpa/217/2000/143

Pfretzschner, H.-U. (2001). Pyrite in fossil bone. *Neues Jahrbuch für Geologie und Paläontologie-Abhandlungen*, 1–23. doi: 10.1127/njgpa/220/2001/1

Pouech, J., Amiot, R., Lécuyer, C., Mazin, J.-M., Martineau, F., and Fourel, F. (2014). Oxygen isotope composition of vertebrate phosphates from Cherves-de-Cognac (Berriasian, France): environmental and ecological significance. *Palaeogeogr. Palaeoclimatol. Palaeoecol.* 410, 290–299. doi: 10.1016/j.palaeo.2014.05.036

Pritchard, P. C. H. (1979). *Encyclopedia of Turtles* (Neptune, NJ: T.F.H. Publications).

Rieppel, O. (2017). *Turtles as hopeful monsters: origins and evolution* (Indiana University Press).

Rieppel, O., and deBraga, M. (1996). Turtles as diapsid reptiles. *Nature* 384, 453–455. doi: 10.1038/384453a0

Rieppel, O., and Reisz, R. R. (1999). The origin and early evolution of turtles. *Annu. Rev. Ecol. Syst.*, 1–22. doi: 10.1146/annurev.ecolsys.30.1.1

Rink, W. J., and Schwarcz, H. P. (1995). Tests for diagenesis in tooth enamel: ESR dating signals and carbonate contents. *J. Archaeological Sci.* 22, 251–255. doi: 10.1006/jasc.1995.0026

Robinson, B. W. (1995). "Variations in the sulfur isotope composition of CDT," in *Reference and intercomparison materials for stable isotopes of light elements, Proceedings of a consultants meeting held in Vienna* (Vienna, Austria: IAEA), 39–45.

Rothschild, B. M. (1987). *Decompression syndrome in fossil marine turtles. Ann. Carnegie Museum* 56, 253–256.

Rothschild, B. M. (1991). Stratophenetic analysis of avascular necrosis in turtles: affirmation of the decompression syndrome hypothesis. *Comp. Biochem. Physiol. Part A: Physiol.* 100, 529–535. doi: 10.1016/0300-9629(91)90365-J

Rothschild, B. M., and Naples, V. (2015). Decompression syndrome and diving behavior in *Odontochelys*, the first turtle. *Acta Palaeontologica Polonica* 60, 163–167.

Rothschild, B. M., and Storrs, G. W. (2003). Decompression syndrome in plesiosaurs (Sauropterygia: Reptilia). *J. Vertebrate Paleontol.* 23, 324–328. doi: 10.1671/0272-4634(2003)023[0324:DSIPSR]2.0.CO;2

Rye, R. O. (2005). A review of the stable-isotope geochemistry of sulfate minerals in selected igneous environments and related hydrothermal systems. *Chem. Geol.* 215, 5–36. doi: 10.1016/j.chemgeo.2004.06.034

Sakai, H., Des Marais, D. J., Ueda, A., and Moore, J. G. (1984). Concentrations and isotope ratios of carbon, nitrogen and sulfur in ocean-floor basalts. *Geochim. Cosmochim. Acta* 48, 2433–2441. doi: 10.1016/0016-7037(84)90295-3

Schoch, R. R., Klein, N., Scheyer, T. M., and Sues, H.-D. (2019). Microanatomy of the stem-turtle *Pappochelys rosinae* indicates a predominantly fossorial mode of life and clarifies early steps in the evolution of the shell. *Sci. Rep.* 9, 1–10. doi: 10.1038/s41598-019-46762-z

Schoch, R. R., and Sues, H.-D. (2015). A Middle Triassic stem-turtle and the evolution of the turtle body plan. *Nature* 523, 584–587. doi: 10.1038/nature14472

Schoch, R. R., and Sues, H.-D. (2020). The origin of the turtle body plan: evidence from fossils and embryos. *Palaeontology* 63, 375–393. doi: 10.1111/pala.12460

Séon, N., Amiot, R., Suan, G., Lécuyer, C., Fourel, F., Demaret, F., et al. (2022). Intra-skeletal variability in phosphate oxygen isotope composition reveals regional heterothermies in marine vertebrates. *Biogeosciences* 19, 2671–2681. doi: 10.5194/bg-19-2671-2022

Shang, Q.-H., and Li, C. (2009). On the occurrence of the ichthyosaur Shastasaurus in the Guanling biota (Late Triassic), Guizhou, China. *Vertebrata PalAsiatica* 47, 178.

Shemesh, A., Kolodny, Y., and Luz, B. (1983). Oxygen isotope variations in phosphate of biogenic apatites, II. Phosphorite rocks. *Earth Planet. Sci. Lett.* 64, 405–416. doi: 10.1016/0012-821X(83)90101-2

Sponheimer, M., and Lee-Thorp, J. A. (2006). Enamel diagenesis at South African Australopith sites: Implications for paleoecological reconstruction with trace elements. *Geochim. Cosmochim. Acta* 70, 1644–1654. doi: 10.1016/j.gca.2005.12.022

Thibon, F., Goedert, J., Séon, N., Weppe, L., Martin, J. E., Amiot, R., et al. (2022). The ecology of modern and fossil vertebrates revisited by lithium isotopes. *Earth Planet. Sci. Lett.* 599, 117840. doi: 10.1016/j.epsl.2022.117840

Trillmich, K. (1979). Feeding behaviour and social behaviour of the marine iguana. *Noticias Galápagos* 29, 19–20.

Trillmich, K. G., and Trillmich, F. (1986). Foraging strategies of the marine iguana, Amblyrhynchus cristatus. *Behav. Ecol. Sociobiol.* 18, 259–266. doi: 10.1007/BF00300002

Vennemann, T. W., Hegner, E., Cliff, G., and Benz, G. W. (2001). Isotopic composition of recent shark teeth as a proxy for environmental conditions. *Geochim. Cosmochim. Acta* 65, 1583–1599. doi: 10.1016/S0016-7037(00)00629-3

Vitousek, M., Rubenstein, D., and Wikelski, M. (2007). "The evolution of foraging behavior in the Galápagos marine iguana: Natural and sexual selection on body size drives ecological, morphological, and behavioral specialization," in *Lizard Ecology*. Eds. S. Reilly, L. McBrayer and D. Miles (Cambridge: Cambridge University Press), 491–507. doi: 10.1017/CBO9780511752438.018

Wang, X., Bachmann, G. H., Hagdorn, H., Sander, P. M., Cuny, G., Xiaohong, C., et al. (2008). The Late Triassic black shales of the Guanling area, Guizhou Province,

south-west China: a unique marine reptile and pelagic crinoid fossil lagerstätte. *Palaeontology* 51, 27–61. doi: 10.1111/j.1475-4983.2007.00735.x

Wheatley, P. V., Peckham, H., Newsome, S. D., and Koch, P. L. (2012). Estimating marine resource use by the American crocodile Crocodylus acutus in southern Florida, USA. *Mar. Ecol. Prog. Ser.* 447, 211–229. doi: 10.3354/meps09503

Wikelski, M., and Trillmich, F. (1994). Foraging strategies of the Galapagos marine iguana (*Amblyrhynchus cristatus*): adapting behavioral rules to ontogenetic size change. *Behaviour* 128, 255–279. doi: 10.1163/156853994X00280

Xafis, A., Sterli, J., Nagel, D., and Vlachos, E. (2018). A basal turtle shows its teeth: possible evidence of dental microwear on the palatal denticles of *Proganochelys quenstedti* (Testudinata; Late Triassic). *Annu. Meeting Palaeontological Association Abstracts* 114.

Zazzo, A., Lécuyer, C., Sheppard, S. M., Grandjean, P., and Mariotti, A. (2004). Diagenesis and the reconstruction of paleoenvironments: a method to restore original $\delta^{18}O$ values of carbonate and phosphate from fossil tooth enamel. *Geochim. Cosmochim. Acta* 68, 2245–2258. doi: 10.1016/j.gca.2003.11.009